2024 European Control Conference (ECC)
June 25-28, 2024. Stockholm, Sweden

Terminal sliding-mode controllers with fixed-time stability and its applications to lateral control of an autonomous vehicle

Moussa Labbadi, Olivier Sename and Vincent Talon

***Abstract*— The stabilization of first and second-order systems in the presence of disturbances has been investigated in this paper. A novel sliding variable is designed utilizing the Gauss error and arctangent functions. This results in a new control rule characterized by its robustness and ease of fixed-time stability implementation. Subsequently, sliding-mode control is applied to achieve the global robust finite-time stabilization of a class of uncertain nonlinear second-order systems. In the simulation, every result is presented. The proposed controller is employed for lateral control of autonomous vehicles. The effectiveness of the suggested method for controlling an autonomous vehicle while considering disturbances is evaluated through nonlinear simulation.**

***Index Terms*— Robust fixed-time stability; sliding mode control; Autonomous vehicles; Lateral Control.**

I. Introduction

Several finite-time controllers have been developed based on various sliding modes [1], terminal sliding mode [2], and integral sliding mode [3] techniques. However, the convergence time of finite-time controllers typically increases unboundedly with the system's initial conditions. Fixed-time stability ensures that the settling time is independent of the initial conditions, in addition to finite-time stability [4], [5], [6], [7], [8]. For engineering applications, fixed-time stabilization offers a predetermined convergence time to the equilibrium, making it a desirable attribute [4], [5], [6], [7], [8]. Specifically, a solution to the singularity problem has been proposed in [4], [5], [6], [7], [8], [9], [11] by employing fixed-time stabilization through the sliding mode control (SMC) technique.

The convergence time of a globally finite-time stable system is constrained and independent of the initial conditions, thanks to fixed-time stability, which is stronger than finite-time stability. This attribute proves particularly beneficial for estimation and optimization in hybrid or switching systems with specific stay times [12]. For the fixed-time stability of nonlinear systems, studies [13]-[15] derive certain Lyapunov characteristics. Additionally, various fixed-time controllers have been developed [3] using the terminal sliding mode manifold. Despite the appealing features of fixed-time controllers mentioned above, tuning the controller gains to achieve convergence within a specific preset settling time is sometimes challenging and, in some cases, impossible. Certain works have recently expanded the application of these findings to second-order systems. An interesting application is in the control of lateral vehicle dynamics: in [16], a fixed-time controller was proposed for autonomous vehicles with saturated input. The lateral control of autonomous systems is a crucial component of autonomous vehicle control [17], [18]. However, designing control systems with a convergence rate for these systems is a challenging task, as indicated by the numerous publications on this topic [17], [18].

This study introduces a novel generic design for achieving fixed-time stability and finite-time stabilization in nonlinear systems subject to matched perturbations. The proposed control scheme ensures fixed-time convergence based on a sliding variable. This sliding variable design incorporates the Gauss error and arctangent functions, which are leveraged to enhance fixed-time stability. Through the utilization of these functions, a new sliding variable is formulated to improve the convergence of the system state. Additionally, it is shown that the closed-loop system achieves global finite-time stability via the application of Lyapunov theory. The theoretical findings are then applied to the lateral control of an autonomous vehicle. The key contributions of this work include: proposal of an accurate and straightforward method for estimating the settling time, which is less complex compared to existing fixed-time stability approaches [9], [10], [19], [20] . Validation of fixed-time regional stability with lower parameter requirements than previous methods [1], simplifying its adjustment. The proposed control strategy is demonstrated in the lateral control of autonomous vehicles in the presence of matched uncertainties.

The notations are introduced in the next section. Based on the Gauss error and arctangent functions, Section II introduces a novel family of fixed-time stability with matched perturbations and its application to robust sliding mode control. The application of the proposed controller is tested on lateral vehicle dynamics (theory and nonlinear simulation), which is presented in Section III. The article is concluded in Section IV.

Notation

The following notations are used. The real numbers set is $\mathbb{R}$; $\mathbb{R}_{>0} = \{z \in \mathbb{R} : z > 0\}$; $\mathbb{R}_{\geq 0} = \mathbb{R}_{>0} \cup \{0\}$; $\mathbb{R}_{\geq 0} = \bar{\mathbb{R}}_{>0} \cup \{\infty\}$. A function $\lambda(z) \in \mathcal{PD}$ (positive definite) if $\lambda : \mathbb{R}_{\geq 0} \to \mathbb{R}_{\geq 0}$ is continuous and $\lambda(0) = 0$, $\lambda(z) > 0$ for all $z > 0$. A function $\lambda : \mathbb{R}_{\geq 0} \to \mathbb{R}_{\geq 0}$ is of class $\mathcal{K}$ (or $\mathcal{K}-$function) if $\lambda \in \mathcal{PD}$ and it is strictly increasing. A

*This work was supported by the ANR (French National Research Agency)

Moussa Labbadi is with the Aix-Marseille University, LIS UMR CNRS 7020, Marseille, France. moussa.labbadi@lis-lab.fr

Olivier Sename is with the Univ. Grenoble Alpes, CNRS, Grenoble INP, GIPSA-lab, 38000 Grenoble, France olivier.sename@grenoble-inp.fr

Vincent Talon is with the TwinswHeel, Designer and manufacturer of logistics droids for factories and cities, 46230 Fontanes, France vincent@twinswheel.fr

scale function $\lambda : \mathbb{R}_{\geq 0} \to [0, 1)$ is of class $\mathcal{K}_1$ if $\lambda \in \mathcal{K}$ and $\lim_{z\to\infty} \lambda(z) = 1$. Then, $\lambda \in \mathcal{DK}_1$ if $\lambda \in \mathcal{K}_1$ and $\lambda \in \mathrm{C}^0$. Let $\mathrm{erf}(z) = \frac{2}{\sqrt{\pi}} \int_0^z \exp\big(-t^2\big)dt$, with $\mathrm{erf}(z)$ is the error function. Finally, let $\mathrm{sgn}(z)$ be a function such that $\mathrm{sgn}(z) = 1$ if $z > 0$, $\mathrm{sgn}(z) \in [-1\,,\,1]$ if $z = 0$, and $\mathrm{sgn}(z) = -1$ if $z < 0$. the error function.

II. Main Results

A. Robust Fixed-time Stability

In this subsection, a robust approach with fixed-time stability is proposed. The main objective of Theorem 1 is to design a new robust fixed-time stability result based on the arctangent and Gauss functions.

Theorem 1: The following system:

$$\begin{cases} \dot{x} = & -\sqrt{\pi}k_1 \left(|\arctan(\mathrm{erf}(x))|\right)^{0.5} \exp\big(x^2\big) \\ & (1 + \mathrm{erf}^2(x))\mathrm{sign}(x) - k_2\mathrm{sign}(x) + d(t), \\ x(0) = & x_0. \end{cases} \tag{1}$$

with $k_1 \in \mathbb{R}^{*+}$, $k_2 \in \mathbb{R}^{*+}$, and $d(t)$ is a perturbation assumed to be bounded as $|d(t)| < \Delta$ with $k_2 > \Delta$, is globally fixed-time stable and the estimate of the settling-time satisfies $T_s(x) \leq \frac{1}{k_1}\sqrt{\frac{\pi}{4}}$,

Proof: Consider the Lyapunov function:

$$V(x) = |x|. \tag{2}$$

Its derivative is given by,

$$\begin{aligned} \dot{V}(x) = &- \big[\sqrt{\pi}k_1 \left(|\arctan(\mathrm{erf}(x))|\right)^{0.5} \exp\big(x^2\big) \\ & (1 + \mathrm{erf}^2(x)) + k_2\big] \,\mathrm{sgn}(x) + d(t)\,\mathrm{sgn}(x) \end{aligned} \tag{3}$$

where $\mathrm{sgn}(x)\,\mathrm{sgn}(x) = 1$. By utilizing $|d(t)| < \Delta$, we obtain

$$\begin{aligned} \dot{V}(x) \leq &- \sqrt{\pi}k_1 \left(|\arctan(\mathrm{erf}(x))|\right)^{0.5} \exp\big(x^2\big)(1 + \mathrm{erf}^2(x)) \\ & - k_2 + \Delta \\ \leq &- \left(|\arctan(\mathrm{erf}(x))|\right)^{0.5} \exp\big(x^2\big) \\ & (1 + \mathrm{erf}^2(x)) \left[\sqrt{\pi}k_1\right] \end{aligned} \tag{4}$$

Using V for $V(x)$ and (2), we have

$$\begin{aligned} \dot{V} \leq &- \left[\sqrt{\pi}k_1\right] \left(|\arctan(\mathrm{erf}(V))|\right)^{0.5} \\ & \exp\big(V^2\big)(1 + \mathrm{erf}^2(V)) \end{aligned} \tag{5}$$

It holds that,

$$\begin{aligned} &\frac{dV}{\left(|\arctan(\mathrm{erf}(V))|\right)^{0.5} \exp(V^2)(1 + \mathrm{erf}^2(V))} \\ &\qquad \leq -[\sqrt{\pi}k_1]dt \end{aligned} \tag{6}$$

and the solution of (6) is $\sqrt{\pi}[\arctan(\mathrm{erf}(x)))^{0.5} - \arctan(\mathrm{erf}(x(0))))^{0.5}] = -[\sqrt{\pi}k_1]t$, then the settling-time is given by:

$$T_s(x) = \frac{(|\arctan(\mathrm{erf}(x(0)))|)^{0.5}}{k_1} \leq \frac{1}{k_1}\sqrt{\frac{\pi}{4}}. \tag{7}$$

It is proved that the settling-time is independent of $x(0)$. ■

The trajectory of the state system (1) and $u(t) = -\sqrt{\pi}k_1(|\arctan(\mathrm{erf}(x))|)^{0.5} \exp\big(x^2\big)\,\mathrm{sgn}(x) - k_2\,\mathrm{sgn}(x)$ with $k_1 = 10$, $k_2 = 6$, and $d(t) = \sin(12t)$, then $\Delta = 1$ and the estimate of the settling-time leads $T_s(x) \leq 0.8$s

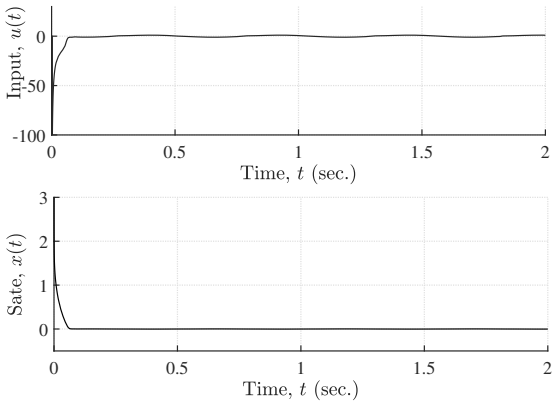

Fig. 1. Illustration of the state x and input $u(t)$.

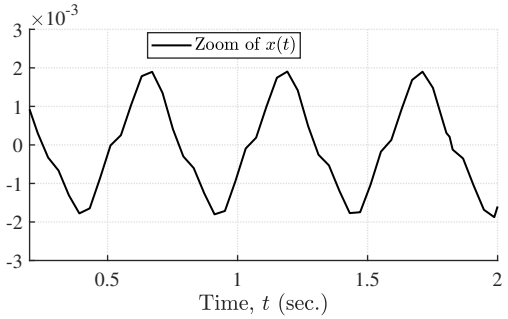

Fig. 2. Illustration of Zoom on the steady state x.

are plotted in Fig. 1. Figure 2 displays the steady state x converging to zero without high oscillation.

Remark 1: The settling-time proved in Theorem 1 depends only on two parameters k_1 and k_2, making it simple and easy to tune.

B. Robust fixed-time sliding mode control

Consider a second order non-linear with uncertainties as:

$$\begin{aligned} \dot{z}_1 &= z_2 \\ \dot{z}_2 &= \varphi_1(z) + \varphi_2(z)u + d(t) \end{aligned} \tag{8}$$

$z_i \in \mathbb{R}$ the state, $\varphi_1(z)$ and $\varphi_2(z)$ are non-linear function satisfying $\varphi_2(z) \neq 0$ and $|d(t)| < \Delta$. Based on Theorem 1 and the induced sliding variable as:

$$\begin{aligned} s_a(z) = &z_2 + \sqrt{\pi}\alpha_3(|\arctan(\mathrm{erf}(z_1))|)^{0.5} \\ & \exp\big(z_1^2\big)(1 + \mathrm{erf}^2(z_1))\,\mathrm{sgn}(z_1) \end{aligned} \tag{9}$$

and the controller,

$$\begin{aligned} u_a(z) = &- \frac{1}{\varphi_2(z)}\big[\varphi_1(z) + \alpha_3((1 + \arctan(\mathrm{erf}(z_1)))\cdot \\ & (\frac{2}{\pi}z_1z_2(1 + (\mathrm{erf}(z_1))^2) + 4\,\mathrm{erf}(z_1))\frac{1}{\sqrt{|\mathrm{erf}(z_1)|}}) \\ & + \sqrt{\pi}\alpha_1(|\arctan(\mathrm{erf}(s_a))|)^{0.5} \exp\big(s_a^2\big) \\ & (1 + \mathrm{erf}^2(s_a))\,\mathrm{sgn}(s_a) + \alpha_2\,\mathrm{sgn}(s_a)\big] \end{aligned} \tag{10}$$

Corollary 1: The system (8) with sliding variable (9) controlled by the law (10) is the global fixed-time stable

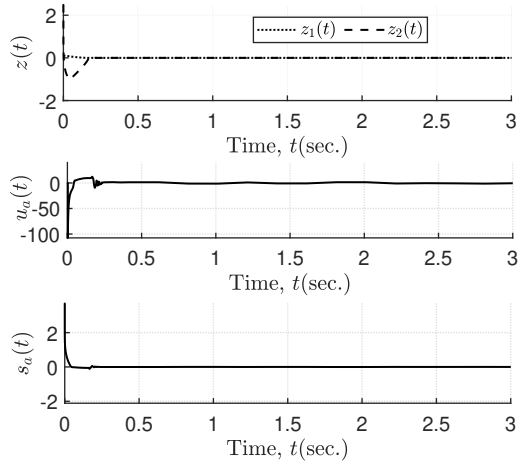

Fig. 3. Top: State variable $z = (z_1(t), z_2(t))$, Center: input $u_a(t)$, Bottom: Sliding variable $s_a(t)$.

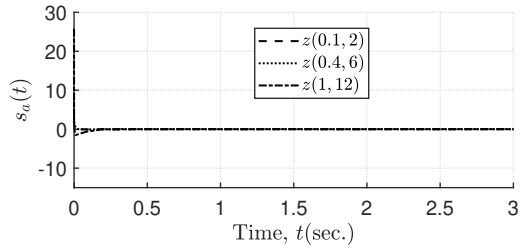

Fig. 4. Sliding variable $s_a(t)$ with different initial conditions.

and the settling-time satisfies

$$T_s(z) \leq \frac{1}{\alpha_1}\sqrt{\frac{\pi}{4}} + \frac{1}{\alpha_3}\sqrt{\frac{\pi}{4}} \tag{11}$$

Proof: Consider the Lyapunov function $V(s_a(t)) = |s_a(t)|$, One has,

$$\begin{aligned}\dot{V}(s_a) =& -\sqrt{\pi}\alpha_1(|\arctan(\mathrm{erf}(s_a))|)^{0.5}\exp\left(s_a^2\right)\\ &(1+\mathrm{erf}^2(s_a)) - \alpha_2 + |d(t)|\\ \leq& -\sqrt{\pi}\alpha_1(|\arctan(\mathrm{erf}(s_a))|)^{0.5}\exp\left(s_a^2\right)\\ &(1+\mathrm{erf}^2(s_a)) - \alpha_2 + \Delta\\ \leq& -(|\arctan(\mathrm{erf}(s_a))|)^{0.5}\exp\left(s_a^2\right)\\ &(1+\mathrm{erf}^2(s_a))[\sqrt{\pi}\alpha_1]\end{aligned} \tag{12}$$

Using Theorem 1, the first part for clossed-loop system (8)-(10) presented in (12) is confirmed and the settling time satisfies $T_{s1}(z_0) \leq \frac{1}{\alpha_1}\sqrt{\frac{\pi}{4}}$. On the other hand, consider the system (9) when $s_a = 0$ as

$$\begin{aligned}\dot{z}_1(z) =& -\sqrt{\pi}\alpha_3(|\arctan(\mathrm{erf}(z_1))|)^{0.5}\exp\left(z_1^2\right)\\ &(1+\mathrm{erf}^2(z_1))\,\mathrm{sgn}(z_1)\end{aligned} \tag{13}$$

Based on the results of Theorem 1, the system (13) reaches their origin in the fixed-time satisfies $T_{s2} \leq \frac{1}{\alpha_3}\sqrt{\frac{\pi}{4}}$. Finally, the robust fixed-time is ensured of the closed-loop system (8)-(10). ■

For the simulation, consider the function $\varphi_1(z) = 0$ and $\varphi_2(z) = 1$, $d(t) = 2\sin(13t)$, the parameters $\alpha_1 = 10, \alpha_2 = 6$, $\alpha_3 = 2$ then $\Delta = 2$ and $z(0) = (z_1(0), z_2(0))$. The evolution of the states, the inputs, and sliding variable are plotted in Fig.3. The evolution of the sliding variable $s_a(t)$ is depicted 4 for different initial conditions. It can be seen that the stabilization time of the sliding variable does not depend on the initial conditions.

Fig. 5. Autonomous Robot ciTHy M (https://www.twinswheel.fr/).

Remark 2: In order to address the singular problem arising in the time derivative of the terminal sliding manifold, several alternative methods can be employed. One such approach involves introducing a tolerance parameter within the sliding surface. This parameter serves to ensure global practical stabilization, thereby avoiding singularity and enabling a regional stability result. This strategy does not necessitate restricting the set of admissible initial conditions, albeit it may result in a reduction in performance.

$$\begin{aligned}s_a(z) =& z_2 + \sqrt{\pi}\alpha_3(|\arctan(\epsilon + \mathrm{erf}(z_1))|)^{0.5}\\ &\exp\left(z_1^2\right)(1+\mathrm{erf}^2(z_1))\,\mathrm{sgn}(z_1)\end{aligned} \tag{14}$$

with $\epsilon > 0$ an arbitrarily small parameter.

III. Application to Lateral Control of an Autonomous Vehicle

The application of the proposed strategy to lateral control of an autonomous vehicle is devoted in this section. The remainder of this section is broken down into three sections. The control oriented model is shown first. A feedback controller is constructed. The outcomes of the real-time simulation are then displayed. The numerical parameters are taken from the SOBEN company of a small four wheels "ciTHy M" range (see Fig. III). This autonomous robot is used for meal distribution and home delivery.

A. Vehicle model and problem formulation

The lateral vehicle behaviour is here stated through the well know bicycle model assuming that the longitudinal speed v_x is constant and explained in [21], [22]. It is represented in Fig. 6 and given by the dynamics equations

$$\dot{v}_y = -v_x r + \frac{1}{m}(F_{yf} + F_{yr} + F_{wy}) \tag{15a}$$

$$\dot{r} = \frac{1}{I_z}(l_f F_{yf} - l_r F_{yr} + l_w F_{wy}) \tag{15b}$$

where the lateral tyre forces of the front and back wheels, respectively, are F_{yf} and F_{yr}. The longitudinal speed is represented by v_x, while the yaw rate is r. The entire mass is m. l_f and l_r represent the front and rear tires' individual distances from the vehicle's mass center, while I_z represents the vehicle's moment of inertia about the yaw axis.

The side wind force F_{wy} is regarded as an external perturbation in this scenario and the tire's lateral slip forces F_{yi} are roughly approximated by linear stiffness with respect to tire slip angles. As a result, the state space representation of the lateral vehicle is provided by

$$\begin{bmatrix}\dot{v}_y\\ \dot{r}\end{bmatrix}=\begin{bmatrix}\overbrace{\underbrace{-2\mu\frac{C_f+C_r}{v_x m}}_{f_3}}^{f_1} & \overbrace{\underbrace{2\mu\frac{-C_f l_f+l_r C_r}{v_x m}-v_x}_{f_4}}^{f_2}\\ \underbrace{2\mu\frac{-l_f C_f+l_r C_r}{v_x I_z}}_{f_3} & \underbrace{-2\mu\frac{C_f l_f^2+l_r^2 C_r}{v_x I_z}}_{f_4}\end{bmatrix}\begin{bmatrix}v_y\\ r\end{bmatrix}+\begin{bmatrix}\overbrace{\underbrace{2\mu\frac{C_f}{m}}_{g_2}}^{g_1}\\ \underbrace{\frac{\mu l_f C_f}{I_z}}_{g_2}\end{bmatrix}\delta+\begin{bmatrix}1\\ l_w\end{bmatrix}F_{wy} \tag{16}$$

The variables and parameters are presented in Table I.

TABLE I

SYSTEM ABBREVIATIONS, NOTATION, AND PARAMETERS.

v_y, v_x	lateral and longitudinal velocities
δ, ψ, r	vehicle steering, yaw angle and yaw rate
y_L, ψ_L	lateral and heading error
ρ, μ	curvature and road friction
m, I_z	mass and z inertia $(160kg, 40kg.m^2)$
C_f, C_r	tires stiffness $(6e3, 5e5)N/rad$
l_f, l_r	wheelbase $(0.8, 0.7)m$
l_w, l_s	preview distance $5m$

In order to handle the lane keeping objective, the heading error ψ_L and the lateral error y_L should converge in fixed-time to zero, the vehicle axis should always be parallel to the planned trajectory tangent axis, and the vehicle lateral deviation should always be close to the nearest trajectory point. The dynamics of both variables are [23]

$$\dot{\psi}_L = r - \rho v_x \tag{17a}$$

$$\dot{y}_L = v_y + \psi_L v_x + r l_s \tag{17b}$$

where ρ stands for the lane's (the reference trajectory's) curvature. For control purpose, the extended model (16)-(17) is considered as in [23].

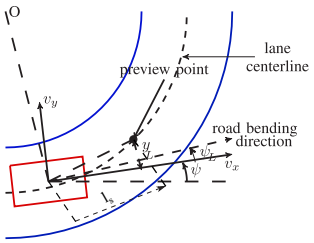

Fig. 6. Graphical definitions of variables y_L and ψ_L in lane keeping cases;

Definition 1: The control issue for lateral motion is shown in the formulation that follows. Find a robust controller that, given the system's (16)-(17) and the time history of the possible road curvature, has the closed-loop features listed below. $\rho(t)$.

P_1) the control effort $\delta(t)$ is bounded and satisfying $\delta(t) \leq \delta_{max}$ and $|\dot{\delta}(t)| \leq v_{max}$.

P_2) the tracking errors converge to zero in fixed-time and the state variables $v_y(t)$ and $r(t)$ converge to their references.

P_3) the closed-loop system with the proposed controller is fixed-time stable.

B. State feedback control law design

In order to develop the lateral controller, the lane keeping and the lateral dynamics of the vehicle are considered as integrated subsystems. This section discusses the application of the fixed-time stability proposed in this paper. Consider the error surface to reduce lane tracking position and orientation errors as:

$$e = c_1 l_p \psi_L + c_2 y_L, \tag{18}$$

Assumption 1: Define a new variable of disturbances as $\Theta(t) = c_2 F_{wy} + l_w F_{wy}(c_1 l_p + c_2 l_s)$, assuming the disturbances $\Theta(t)$ is bounded and $|\Theta(t)| \leq \hbar$.

where c_1 and c_2 are positive coefficients. Given that a terminal sliding surface has a relative degree of 2 of the error being considered, it can be defined as:

$$\begin{aligned} s(e) =& \dot{e}(t) + \sqrt{\pi}\kappa_1(|\arctan(\epsilon + \operatorname{erf}(e))|)^{0.5} \\ & \exp\left(e^2\right)(1+\operatorname{erf}^2(e))\operatorname{sgn}(e) \end{aligned} \tag{19}$$

and the controller is chosen as:

$$\begin{aligned} \delta =& -\frac{1}{\varphi_a}[\varphi_b + \kappa_1((1+\arctan(\operatorname{erf}(e))) \\ & (\frac{2}{\pi}e\dot{e}(1+(\operatorname{erf}(e))^2)+4\operatorname{erf}(e))\frac{1}{\sqrt{\epsilon+|\operatorname{erf}(e)|}}) \\ & + \sqrt{\pi}\kappa_3(|\arctan(\operatorname{erf}(s))|)^{0.5}\exp\left(s^2\right) \\ & (1+\operatorname{erf}^2(s))\operatorname{sgn}(s) + \kappa_2\operatorname{sgn}(s)] \end{aligned} \tag{20}$$

with $\varphi_a = (c_1 l_p + c_2 l_s)g_2 + c_2 g_1$ and $\varphi_b = (c_1 l_p + c_2 l_s)g_2 + c_2 g_1 c_2(f_1 v_y + f_2 r) + (c_1 l_p + c_2 l_s)(f_3 v_y + f_4 r) - c_1 l_p \dot{\rho} v_x + c_2 \dot{\psi}_L v_x$.

Corollary 2: Consider the dynamical lateral in *qre-flinearsystem with the perturbation* $\Theta(t)$*, then the closed-loop lateral extended system* (16)*,* (17)*,* (19)*, and* (20) *is globally fixed-time stable and the settling-time satisfies*

$$T_s \leq \frac{1}{\kappa_3}\sqrt{\frac{\pi}{4}} + \frac{1}{\kappa_1}\sqrt{\frac{\pi}{4}} \tag{21}$$

Proof: Consider the Lyapunov function $V(s(t)) = |s(t)|$, Its derivative given by,

$$\begin{aligned} \dot{V}(s) =& -\sqrt{\pi}\kappa_3(|\arctan(\operatorname{erf}(s))|)^{0.5}\exp\left(s^2\right)(1+\operatorname{erf}^2(s)) \\ & -\kappa_2 + |\Theta(t)| \\ \leq& -\sqrt{\pi}\kappa_3(|\arctan(\operatorname{erf}(s))|)^{0.5}\exp\left(s^2\right)(1+\operatorname{erf}^2(s)) \\ & -\kappa_2 + \hbar \\ \leq& -(|\arctan(\operatorname{erf}(s))|)^{0.5}\exp\left(s^2\right)(1+\operatorname{erf}^2(s)) \\ & [\sqrt{\pi}\kappa_3 + (\kappa_2 - \hbar)] \end{aligned} \tag{22}$$

Using Theorem 1, the first part of system (22) is confirmed with the settling time satisfies $T_{s1}(e) \leq \frac{1}{\kappa_3}\sqrt{\frac{\pi}{4}}$. For $\{s(0) = 0\}$, we can obtain $T_{s2}(s_0) \leq \frac{1}{\kappa_1}\sqrt{\frac{\pi}{4}}$ by using the same steps

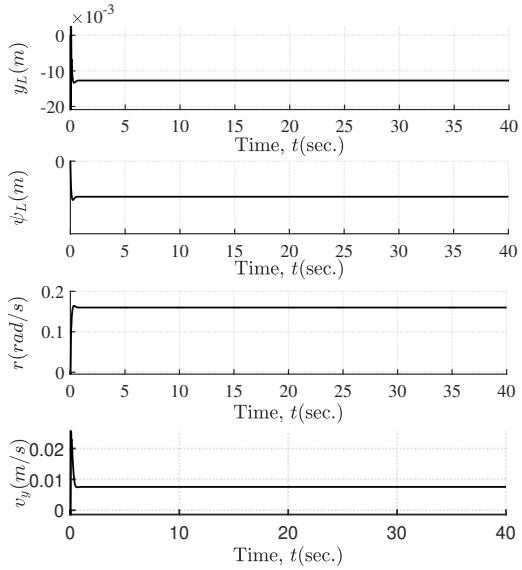

Fig. 7. Case 1: Illustration of the lateral deviation y_L, heading error ψ_L, yaw rate r and lateral speed v_y.

given in the proof of Theorem 1, then the robust global fixed-time is ensured of the lateral closed-loop system. ■

C. Validation on droid delivery manufacturer ("twinswheel ciTHy M") using real data

In this section, a nonlinear simulation based on a 7-degree-of-freedom (DOF) model is employed. The model encompasses yaw rotations, longitudinal and lateral displacements, as well as four-wheel rotations with tire longitudinal slip. This simulation aims to demonstrate the effectiveness of the developed control strategy through scenarios involving uniform circular motion and real trajectory data.

Remark 3: Due to discontinuous input, we encounter the chattering problem. To mitigate this issue, the tangent function has been employed as a substitute for the signum function.

The external disturbance represents the resistive wind force using the equation $F_{wy} = c_y v_x^2$. The parameter values for the "ciTHy M" robot in each simulation are also included in Table I. Two simulation cases are used as:

- Case 1
  It should be emphasized that we assume we drive the car at a constant forward speed of $v_x = 8m/s$. In this section, we consider the trajectory's curvature to be constant, specifically set to $\rho(t) = 0.02$. This implies that the vehicle is controlled to follow a circular path. We introduce an abrupt change in the reference trajectory to transition to a circle with a radius of 50 meters. The simulation results, depicted in Figs. 7 and 8, showcase the performance of the suggested control strategies. These figures illustrate how effectively the proposed strategies manage to control the system. All four critical variables associated with the lateral dynamics of the vehicle converge to their respective reference values, underscoring the effectiveness of the suggested control approach. Moreover, both controllers demonstrate the capability to accurately track the reference path even in scenarios where the path's curvature remains constant. This robust performance highlights the efficacy of the control strategies under consideration.
- Case 2

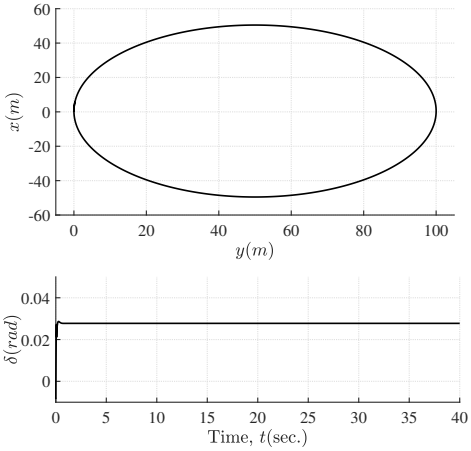

Fig. 8. Case 1: Illustration of the steering control and xy trajectory.

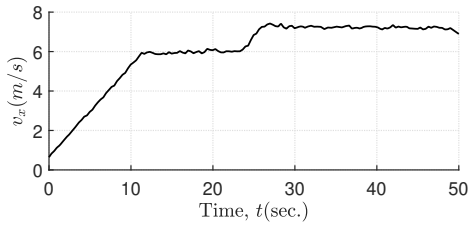

Fig. 9. Case 2: Real longitudinal velocity profile.

The data-set containing the trajectory information was collected experimentally from the "ciTHy M" robot on a test track in Cahors, France. In this case, the robot is put through the road map curvature and longitudinal speed, with the measured experimental results shown respectively in Figs. 9 and 10. The robot enters autonomous mode at $0.2m/s$ with a $0m$ initial lateral error. Then, the robot accelerates to $6m/s$ and then accelerates again to $7m/s$. Figure 11 shows the results of the lateral offset, heading orientation, yaw rate and lateral speed. It can be seen that the proposed controller is able to sustain a good tracking performance since the maximum lateral deviation and heading orientation never get respectively more than $0.02m$ and $0.05rad$. Figure 12 shows

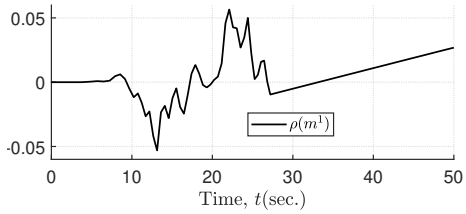

Fig. 10. Case 2: Road map curvature.

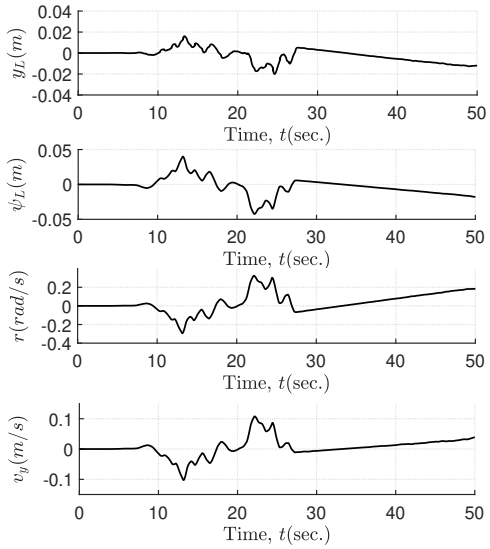

Fig. 11. Case 2: Illustration of the lateral deviation y_L, heading error ψ_L, yaw rate r and lateral speed v_y.

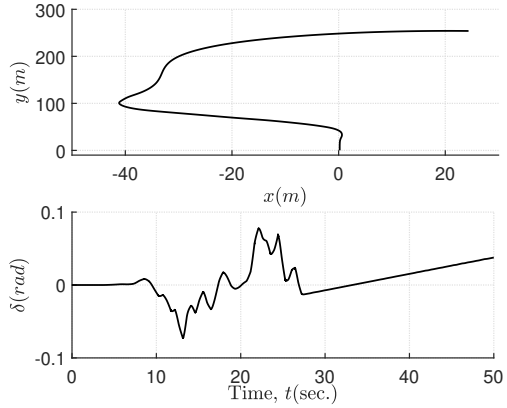

Fig. 12. Case 2: Illustration of the steering control and xy trajectory.

the trajectory tracking and the applied steering control. This later is smooth without chattering problem and has small value.

IV. Conclusions

The paper proposed a new robust fixed-time stability and fixed-time stabilization using Gauss error and arctangent functions. The proposed fixed-time stability has been exploited for a class of uncertain nonlinear second-order systems. Then, this strategy was used for the lateral control of an autonomous vehicle system. This approach has been proven to be a suitable option for managing such systems and ensuring the needed tracking. Additionally, testing on a real-time simulation platform has demonstrated how well the suggested technique performs.

Acknowledgement

The authors gratefully acknowledges the financial support from the ANR (French National Research Agency) through the project by FRANCE RELANCE Grenoble INP-SOBEN

References

[1] Utkin, Vadim I. Sliding modes in control and optimization. Springer Science & Business Media, 2013.
[2] Wu, Yuqiang, Xinghuo Yu, and Zhihong Man. "Terminal sliding mode control design for uncertain dynamic systems." Systems & Control Letters 34.5 (1998): 281-287.
[3] Rubagotti, Matteo, et al. "Integral sliding mode control for nonlinear systems with matched and unmatched perturbations." IEEE Transactions on Automatic Control 56.11 (2011): 2699-2704.
[4] M. Labbadi, G. P. Incremona and A. Ferrara, "Design of an Easy-to-Implement Fixed-Time Stable Sliding Mode Control," in IEEE Control Systems Letters, doi: 10.1109/LCSYS.2023.3327235.
[5] Y. Liu, H. Li, R. Lu, Z. Zuo and X. Li, "An Overview of Finite/Fixed-Time Control and Its Application in Engineering Systems," in IEEE/-CAA Journal of Automatica Sinica, vol. 9, no. 12, pp. 2106-2120, Dec. 2022.
[6] Aldana-L'opez, Rodrigo, et al. "Generating new classes of fixed-time stable systems with predefined upper bound for the settling time." International Journal of Control 95.10 2802-2814, 2022.
[7] Aldana-L'opez, Rodrigo, et al. "Enhancing the settling time estimation of a class of fixed-time stable systems." International Journal of Robust and Nonlinear Control 29.12 : 4135-4148, 2019.
[8] E. Jim'enez-Rodr'iguez, A. J. Mu ñoz-V'azquez, J. D. S'anchez-Torres, M. Defoort and A. G. Loukianov, "A Lyapunov-Like Characterization of Predefined-Time Stability," in IEEE Transactions on Automatic Control, vol. 65, no. 11, pp. 4922-4927, Nov. 2020.
[9] Zuo, Zongyu. "Nonsingular fixed-time terminal sliding mode control of non-linear systems." IET control theory & applications 9.4 (2015): 545-552.
[10] Corradini, Maria Letizia, and Andrea Cristofaro. "Nonsingular terminal sliding-mode control of nonlinear planar systems with global fixed-time stability guarantees." Automatica 95 (2018): 561-565.
[11] A Ferrara, Antonella, and Gian Paolo Incremona. "Predefined-time output stabilization with second order sliding mode generation." IEEE Transactions on Automatic Control 66.3 (2020): 1445-1451.
[12] Tian, Bailing, et al. "A fixed-time output feedback control scheme for double integrator systems." Automatica 80 (2017): 17-24.
[13] R. Aldana-López , D. Gómez-Gutiérrez , E. Jiménez-Rodríguez , J.D. Sánchez-Torres , M. Defoort , "Enhancing the settling time estimation of a class of fixed-time stable systems", Int. J. Robust Nonlinear Control 29 (12) (2019) 4135-4148.
[14] Lopez-Ramirez, Francisco, et al. "Conditions for fixed-time stability and stabilization of continuous autonomous systems." Systems & Control Letters 129 (2019): 26-35.
[15] Polyakov, Andrey. "Nonlinear feedback design for fixed-time stabilization of linear control systems." IEEE Transactions on Automatic Control 57.8 (2011): 2106-2110.
[16] Zhang, Xinrong, et al. "Path tracking control for autonomous vehicles with saturated input: A fuzzy fixed-time learning control approach." IET Intelligent Transport Systems 16.4 (2022): 531-542.
[17] Z. Liang, Z. Wang, J. Zhao, P. K. Wong, Z. Yang and Z. Ding, "Fixed-Time Prescribed Performance Path-Following Control for Autonomous Vehicle With Complete Unknown Parameters," in IEEE Transactions on Industrial Electronics, vol. 70, no. 8, pp. 8426-8436, Aug. 2023
[18] Z. Liang, M. Shen, Z. Li and J. Yang, "Model-Free Output Feedback Path Following Control for Autonomous Vehicle With Prescribed Performance Independent of Initial Conditions," in IEEE/ASME Transactions on Mechatronics, doi: 10.1109/TMECH.2023.3293100.
[19] Moulay, Emmanuel, et al. "Robust fixed-time stability: Application to sliding-mode control." IEEE Transactions on Automatic Control 67.2 (2021): 1061-1066.
[20] Huijie Li and Yuanli Cai. Fixed-time non-singular terminal sliding mode control with globally fast convergence. IET Control Theory & Applications, 2022.
[21] Jiang, Jingjing, and Alessandro Astolfi. "Lateral control of an autonomous vehicle." IEEE Transactions on Intelligent Vehicles 3.2 (2018): 228-237.
[22] R. Rajamani, Vehicle Dynamics and Control. New York, NY, USA: Springer, 2012.
[23] Kapsalis, Dimitrios, et al. "A reduced LPV polytopic look-ahead steering controller for autonomous vehicles." Control Engineering Practice 129 (2022): 105360.